ELSEVIER

Journal of Photochemistry and Photobiology A: Chemistry 141 (2001) 33–38

Journal of Photochemistry and Photobiology A:Chemistry

www.elsevier.nl/locate/jphotochem

Decay kinetics of photosensitized triplet crystal violet in acetonitrile

Yousry M.A. Naguib [a], Colin Steel [b,*], Michael A. Young [c]

[a] *Faculty of Education, Suez Canal University, El-Arish, Egypt*
[b] *Department of Chemistry, Brandeis University, Waltham, MA 02254, USA*
[c] *Polaroid Corporation, Cambridge, MA 02139, USA*

Received 27 November 2000; received in revised form 6 March 2001; accepted 12 March 2001

Abstract

Triplet excited state crystal violet ($^3CV^+$) was produced in acetonitrile via triplet sensitization by anthracene (An) which was excited by Nd:YAG laser at 355 nm. The kinetics of the formation and decay of $^3CV^+$ were mostly studied by monitoring the bleach and recovery of CV^+ at 590 nm (the absorbance maximum). This allows the determination of the percentage of quenching of triplet anthracene by crystal violet by electron transfer to yield radicals (reaction 3b, 13%) as opposed to energy transfer to yield $^3CV^+$ (reaction 3a, 87%). The $^3CV^+$ so formed returns to the ground state by a first-order process (4) and also by reaction with ground state CV^+ (6). There are two channels for the latter reaction. One is direct reversion to the ground state (6a), the other is electron transfer resulting in radical formation (6b).

The crystal violet radicals formed in both electron-transfer processes ultimately revert to CV^+ resulting in a very low yield for triplet-sensitized consumption of CV^+. The rate constants and branching parameters for the elementary processes in the reaction scheme were determined. The absorbance changes during the bleach and recovery were also monitored at 520, 540, 560, and 605 nm. The absorbance ratios for these wavelengths relative to 590 nm, during the bleach and recovery were the same as for CV^+ absorption, suggesting that depopulation of $^3CV^+$ results in rapid reversion to normal CV^+ ground state conformation.

Keywords: Crystal violet; Anthracene; Energy transfer; Electron transfer; Reaction mechanism

1. Introduction

The photophysics and photochemistry of triarylmethane dyes (D^+) have received much attention in recent years with respect to the nature of the excited states and the mechanism of their light stability in liquid and solid media, and have been reviewed [1].

Triarylmethane dyes such as crystal violet (CV^+) exhibit intense visible absorption bands, yet in solvents of normal viscosity, they show very little fluorescence due to rapid non-radiative decay from the first excited singlet to the ground state in a few picoseconds bypassing the triplet manifold [2–6]. The quantum yields of fluorescence and singlet excited lifetime are strongly solvent dependent [1]. Forster and Hoffman [7] proposed that excitation of D^+ results in a conformational change to a new equilibrium position, brought about by a synchronous rotation of aryl groups, characterized by a high rate of radiationless relaxation. The viscous drag of the solvent hinders this rotation, and the increasing solvent viscosity results in high fluorescence yield. Using ground state absorption recovery technique Sundstrom and coworkers [5] obtained a double exponential decay for the lifetime of $^1D^+$. They attributed their results to a twisted excited state conformation characterized by solvent dependent recovery rates. Vogel and Rettig [6] who also measured fluorescence yields as a function of solvent viscosity and temperature offered a similar proposal.

In accordance with these photo-physical studies, we previously reported [8] that the quantum yields for photo-bleaching of CV^+ in solvents of low viscosity such as 2-propanol and acetonitrile by direct excitation in the visible are indeed very low, $\leq 10^{-7}$.

The photo-physical studies indicate that the fluorescence and intersystem crossing yields could be enhanced when rotation of aryl groups is impeded, and the molecular mobility is restricted. Indeed, several studies [1] have shown that excitation of D^+ in the visible resulted in phosphorescence emissions in the red and infrared when D^+ was either incorporated into a glass matrix or bound to a high molecular weight polymer. The red phosphorescence and a metastable state, presumed to be the triplet, absorbing at 480 nm for CV^+ and obtained by flash photolysis of CV^+ bound to a polymer, were correlated with the ability of bound CV^+ to undergo photoreduction [9]. Nouchi and Silvie [10] have measured the triplet–triplet absorption of CV^+, which

* Corresponding author.
E-mail address: steel@brandeis.edu (C. Steel).

1010-6030/01/$ – see front matter
PII: S1010-6030(01)00428-2

displayed a band near 625 nm and a weaker band in the IR at 1250 nm, and related dyes in Plexiglass at 77 K.

Leaver [11] observed the triplet ESR signal of CV^+ in aqueous ethylene glycol at 90 K, and reported the phosphorescence of $^3CV^+$ occurred at $\lambda_{max} = 730$ nm with lifetime of 0.29 s. Jones and Goswami [12], employing flash photolysis technique on CV^+ bound to polymethacrylic acid, observed a transient absorbing at 460 nm ($\varepsilon = 1.1 \times 10^4\,M^{-1}\,cm^{-1}$) and 640 nm (weak) which was assigned to $^3CV^+$. They were also able to detect the formation of $CV^\bullet$ and $CV^{\bullet 2+}$ which absorb at 410 and 600 nm, respectively, produced on electron transfer between the bound dye and co-bound electron donor and acceptors.

We wished to ascertain the behavior of $^3CV^+$ in a conventional solvent (acetonitrile). Since $^1CV^+$ does not undergo significant intersystem crossing, the most convenient method for producing $^3CV^+$ is triplet sensitization, a method we had previously employed [13]. We decided to use anthracene (An) as the sensitizer and to follow the bleach and recovery of ground state CV^+ at 590 nm. (a) The triplet energy (E_T) of anthracene is greater than that of CV^+. (b) Neither anthracene nor its triplet absorb at 590 nm, where the sensitized bleach and recovery of CV^+ can be readily followed. (c) Although there is considerable uncertainty as to the exact regions for absorption of intermediates such as $^3CV^+$, $CV^\bullet$ and $CV^{\bullet 2+}$, we observed no significant interference of intermediate species at 590 nm, where CV^+ absorbs strongly ($\varepsilon_{590} = 0.97 \times 10^5\,M^{-1}\,cm^{-1}$).

2. Experimental

Crystal violet chloride (Aldrich) was recrystallized from water and anthracene (Pilot scintillation grade) was used as received. All samples (3 ml) were prepared using acetonitrile as solvent and were degassed by freeze-thaw cycles at 10^{-5} Torr. For kinetic bleach and recovery experiments, the anthracene sensitizer concentration (1.01×10^{-5} M) was chosen to give an absorbance of 0.078 in a 1 cm path-length quartz cell. The degassed samples were excited with a single unfocused 355 nm, ≈6 mJ pulse from a frequency-tripled Molectron YAG laser. At 355 nm the extinction coefficient of anthracene is $7770\,M^{-1}\,cm^{-1}$. The resulting transient absorption was detected and processed as previously described [13]. Measurement of the transient bleach and recovery at 590 nm was started 0.25 μs after the flash, by which time transient scatter from the flash was over.

The absorption spectrum of triplet anthracene (^3An) in the 380–460 nm range was obtained using an EG&G PAR OMA2 multi-channel detection system with a 1 μs delay between laser excitation and detection. The known extinction coefficient at 418 nm allowed the initial ^3An concentration both in the absence and presence of CV^+ to be determined. In the latter case, since CV^+ absorbs weakly at 355 nm — $\varepsilon_{355} = 3020\,M^{-1}\,cm^{-1}$, a small inner filter correction was applied. The ^3An decay in the absence of CV^+ (Section 3.1) was followed at 418 nm.

3. Results and discussion

3.1. Triplet anthracene decay

The decay of triplet anthracene (^3An) can be accounted for by the following two equations:

$$^3An \xrightarrow{k_1} An \quad (1)$$

$$2\,^3An \xrightarrow{k_2} 2An \quad (2)$$

The second reaction is triplet–triplet annihilation, while the first represents all pseudo-first-order decays. In previous work we showed that for rigorously purified solvents and after extensive out-gassing k_1 could be $\leq 150\,s^{-1}$ for ^3An in pyridine and in hexane [14]. Generally this value is larger because of trace residual O_2 and trace impurities in the solvent. So, it is best to simply measure this parameter in any experimental system, and accept it as an empirical value. In this study by following the decay of ^3An, obtained by laser excitation at 355 nm of 1.01×10^{-5} M anthracene in acetonitrile, we found $k_1 = (5200 \pm 1500)\,s^{-1}$ (80% confidence) and $k_2 = (5.2 \pm 0.5) \times 10^9\,M^{-1}\,s^{-1}$ (80% confidence). The latter is a value close to that given in the literature ($k_2 = 8 \times 10^9\,M^{-1}\,s^{-1}$ in hexane [15]). The extinction coefficient of ^3S at 418 nm was taken to be $64{,}700\,M^{-1}\,cm^{-1}$, which is the literature value obtained in cyclohexane [16].

3.2. Quenching of triplet anthracene by crystal violet

3.2.1. Crystal violet quenching constant (k_3)

Sensitizers whose triplet energies (E_T) are greater than the E_T of the triaryl methane (TAM) dye are quenched efficiently by that TAM dye. This includes ^3An ($E_T = 43$ kcal/mol) [17] and the TAM dye crystal violet (CV^+, $E_T = 39$ kcal/mol) [18]. The quenching is most readily followed by monitoring the bleaching of the CV^+ absorption at its absorption maximum (590 nm, $\varepsilon(CV^+) = 0.97 \times 10^5\,M^{-1}\,cm^{-1}$).

We have previously interpreted this quenching as arising from triplet transfer to CV^+

$$^3An + CV^+ \xrightarrow{k_3} An + {}^3CV^+ \quad (3)$$

Bhasikuttan et al. [19] have studied the same reaction using benzene as solvent. They also interpreted their results in terms of 100% triplet transfer. Fig. 1 shows the bleaching of CV^+ over the first 9 μs at four different concentrations of CV^+, whilst Figs. 2 and 3 show data over 100 μs. We shall concentrate first on Fig. 1.

Experimental absorbance changes at 590 nm ($\Delta A_{exp,t}$), defined by

$$\Delta A_{exp,t} = A_t - A_0$$

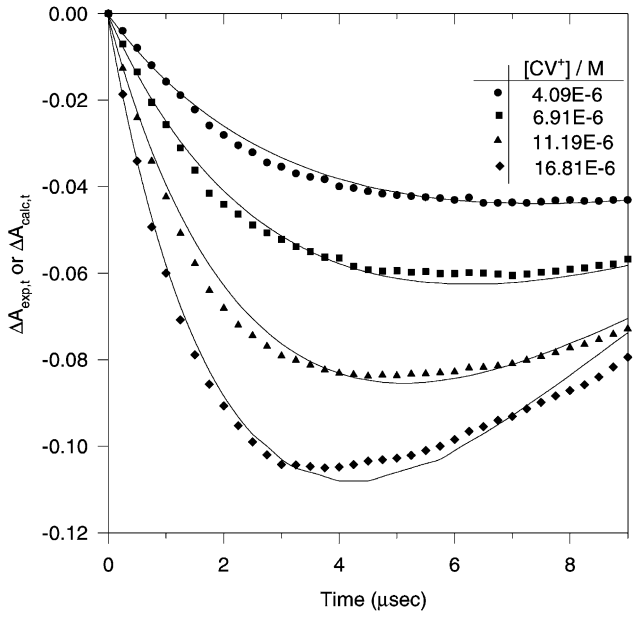

Fig. 1. First 9 μs of the anthracene-sensitized bleach and recovery of crystal violet monitored at 590 nm in acetonitrile. The anthracene concentration was 1.01×10^{-5} M; the crystal violet concentrations are shown in the inset. The points are the experimental values. The full line curves are the preliminary model values using known constants $k_1 = 5200\,s^{-1}$, $k_2 = 5.2 \times 10^9\,M^{-1}\,s^{-1}$, $k_3 = 1.84 \times 10^{10}\,M^{-1}\,s^{-1}$. Assumed constant $k_5 = 1 \times 10^{10}\,M^{-1}\,s^{-1}$. Variable parameters $k_4 = 1.8 \times 10^5\,s^{-1}$, $k_6 = -1.7 \times 10^9\,M^{-1}\,s^{-1}$.

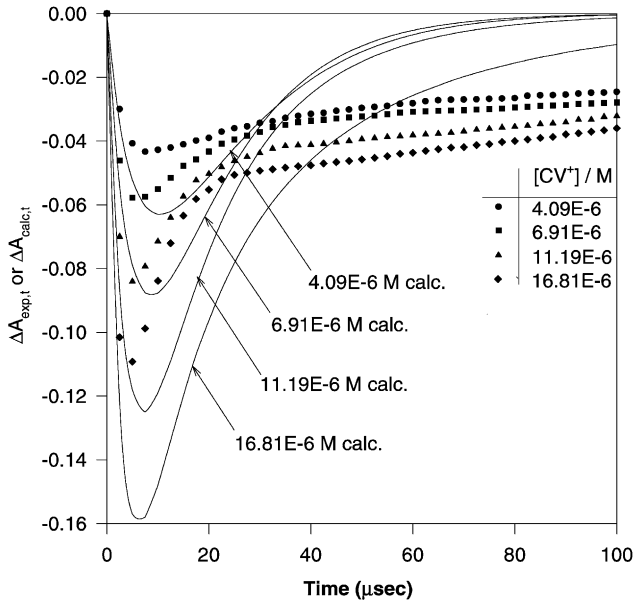

Fig. 2. Anthracene-sensitized bleach and recovery of crystal violet monitored at 590 nm in acetonitrile over 100 μs. Same conditions as for Fig. 1, but now the best variable parameters are $k_4 = 9.8 \times 10^4\,s^{-1}$, $k_6 = -4.6 \times 10^9\,M^{-1}\,s^{-1}$.

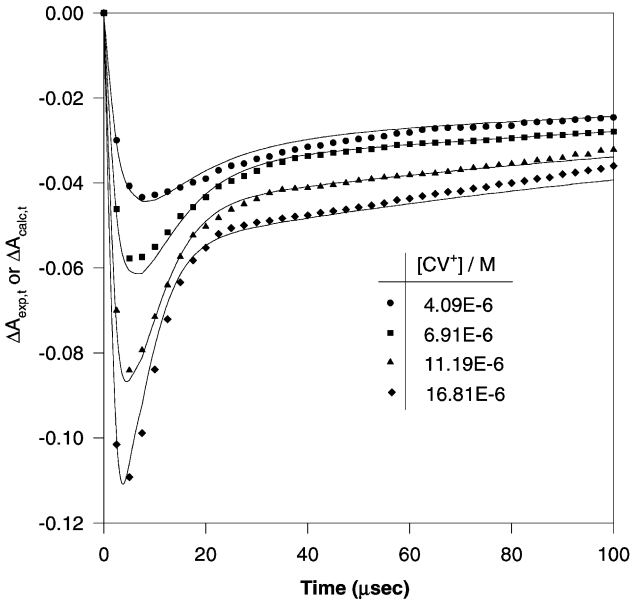

Fig. 3. Anthracene-sensitized bleach and recovery of crystal violet monitored at 590 nm in acetonitrile. The model now includes electron transfer k_1, k_2, k_3, k_5 as in Figs. 1 and 2. Assumed constants $k_7 = k_8 = 1 \times 10^{10}\,M^{-1}\,s^{-1}$, $\alpha = \beta = 0.5$. Best-fit variable parameters $\sigma = 0.88$, $k_4 = 2.3 \times 10^5\,s^{-1}$, $k_6 = 2.0 \times 10^9\,M^{-1}\,s^{-1}$.

where A_t and A_0 are the CV^+ absorbances at times t and 0, were recorded every 0.25 μs. The digital slope between adjacent points is

$$\frac{\Delta A_{\text{exp}}(i+1) - \Delta A_{\text{exp}}(i)}{2.5 \times 10^{-7}}$$

Initial slopes, $(d\Delta A_{\text{exp}}/dt)_0$, at each concentration were then determined by carrying out regression analysis on the digital slopes obtained over the first 3 μs.

The rate constant k_3 is found from

$$\left(\frac{d\Delta A_{\text{exp}}}{dt}\right)_0 = k[^3\text{An}]_0 A_0$$

Initial triplet anthracene concentrations, $[^3\text{An}]_0$ were determined by measuring the peak transient absorbances at 418 nm, where $\varepsilon(^3\text{An}) = 64{,}700\,M\,cm^{-1}$.

In this way, we found $k_3 = 1.84 \pm 0.15 \times 10^{10}\,M^{-1}\,s^{-1}$ (80% confidence level). This result agrees nicely with a previous determination [13]. For convenience, the measured parameters are gathered together in Table 1.

Table 1
Experimentally measured rate constants

Rate constant	Value
k_1 (s^{-1})	$(5.2 \pm 1.5) \times 10^3$
k_2 ($M^{-1}\,s^{-1}$)	$(5.2 \pm 0.5) \times 10^9$
k_3 ($M^{-1}\,s^{-1}$)	$(1.84 \pm 0.15) \times 10^{10}$

3.3. Mechanism of bleaching and recovery of crystal violet

Kinetics of formation and decay of $^3CV^+$ were studied by monitoring the bleaching and ground state recovery of CV^+ at 590 nm. The technique of ground state recovery has been employed extensively to study the dynamics of the short lived singlet excited states of D^+ [1]. The wavelength 590 nm was chosen to monitor the bleach and recovery of CV^+. (a) CV^+ has its highest extinction coefficient ($0.97 \times 10^5\ M^{-1}\ cm^{-1}$) at 590 nm in acetonitrile. (b) Anthracene and its triplet excited state show no absorption at 590 nm. (c) Various other species $An^{\bullet+}$ [20], $^3CV^+$, CV and $CV^{\bullet 2+}$ do not absorb appreciably at 590 nm, see Section 1. (d) The ratio of absorbances at 520, 540, 560, and 605–590 nm for the bleached transient at different times between 4 and 90 μs closely resembles the corresponding ratios for ground state CV^+, indicating that no other species absorb appreciably in this region.

3.3.1. 0–9 μs data

Triplet anthracene sensitized quantum yield of consumption of CV^+ is very low, ${}^{An}\Phi(-CV^+) = 1.1 \times 10^{-5}$ [13]. This means that the $^3CV^+$ formed in reaction (3) must finally return to ground-state CV^+. The simplest way to accommodate this fact is to assume that $^3CV^+$ undergoes reactions analogous to (1) and (2).

$$^3CV^+ \xrightarrow{k_4} CV^+ \tag{4}$$

$$2\,^3CV^+ \xrightarrow{k_5} 2CV^+ \tag{5}$$

We also include possible quenching of $^3CV^+$ by CV^+

$$^3CV^+ + CV^+ \xrightarrow{k_6} 2CV^+ \tag{6}$$

The differential rate equations representing reactions (1)–(6) may be numerically integrated to determine calculated values for the crystal violet concentration as a function of time, $[CV^+]_{calc,t}$, and hence $\Delta A_{calc,t}$ for those times at which there is experimental data ($\Delta A_{exp,t}$). To begin with, it is reasonable to assume that the triplet–triplet annihilation reaction (5) is close to diffusion controlled [15], see also reaction (2). Thus, only k_4 and k_6 are unknowns.

For any given set of values ($k_1, \ldots, k_6$), the standard deviation in ΔA_{exp} about the regression ($s_{\Delta A}$) may be obtained

$$s_{\Delta A} = \sqrt{\frac{\sum_i (\Delta A_{calc}(i) - \Delta A_{exp}(i))^2}{N - m}}$$

where the summation is over all N data points for the four concentrations and m is the number of unknown parameters. Using a simplex procedure [21,22], our data-fitting program varied the unknown parameters (in this case k_4 and k_6), and numerically integrated the differential equations to determine a new set of $\Delta A_{calc}(i)$ for each iteration until a minimum for $s_{\Delta A}$ was reached. This gives "best" k_4 and k_6. Although a fair fit to the data over the first 9 μs could be obtained with reasonable positive values for k_4 and k_6, the best-fit (shown in Fig. 1 was actually obtained with a *negative* value ($-1.7 \times 10^9\ M^{-1}\ s^{-1}$) for k_6.

3.3.2. 0–100 μs data

The situation becomes even worse when we try to fit the full 0–100 μs data (Fig. 2). Not only do reasonable parameters give a poor fit. Even the best-fit parameters for k_4 and k_6 give a poor fit, and the best-fit k_6 is once again negative.

The picture becomes dramatically better when the quenching process is expanded to include electron transfer, Fig. 3. Reaction (3) now becomes

$$^3An + CV^+ \underset{\sigma}{\xrightarrow{k_3}} An + {}^3CV^+ \tag{3a}$$

$$^3An + CV^+ \underset{1-\sigma}{\xrightarrow{k_3}} An^{\bullet+} + CV^{\bullet} \tag{3b}$$

where σ is the fraction going by energy transfer and $(1-\sigma)$ the fraction proceeding by electron transfer. Reactions (5) and (6) have also been expanded to include the possibility that fractions α and β proceed by electron transfer

$$2\,^3CV^+ \underset{1-\alpha}{\xrightarrow{k_5}} 2CV^+ \tag{5a}$$

$$2\,^3CV^+ \underset{\alpha}{\xrightarrow{k_5}} CV^{\bullet} + CV^{\bullet 2+} \tag{5b}$$

$$^3CV^+ + CV^+ \underset{1-\beta}{\xrightarrow{k_6}} 2CV^+ \tag{6a}$$

$$^3CV^+ + CV^+ \underset{\beta}{\xrightarrow{k_6}} CV^{\bullet} + CV^{\bullet 2+} \tag{6b}$$

To accommodate the fact that the overall yield of triplet sensitized decomposition is very low, the CV-derived radicals formed in (5b) and (6b) have to revert to CV^+, so we also add the radical–radical reactions

$$CV^{\bullet} + CV^{\bullet 2+} \xrightarrow{k_7} 2CV^+ \tag{7}$$

$$CV^{\bullet} + An^{\bullet+} \xrightarrow{k_8} CV^+ + An \tag{8}$$

Let us start by assuming that the last two reactions occur at close to their diffusion-controlled values ($k_7 = k_8 = 1 \times 10^{10}\ M^{-1}\ s^{-1}$), and arbitrarily set $\alpha = \beta = 0.5$. The unknown and variable parameters are then k_4, k_6 and σ. The best-fit curves are shown in Fig. 3. Not only is the initial bleach and recovery quantitatively replicated, but the long-time slow recovery is also well modeled. Moreover, the best-fit values for k_4 ($=2.3 \times 10^5\ s^{-1}$) and k_6 ($=2.0 \times 10^9\ M^{-1}\ s^{-1}$) are reasonable. Efficient quenching of a triplet dye by its ground state has previously been reported [23]. The best-fit value of σ is 0.88, indicating that although energy transfer is indeed the major quenching reaction, electron transfer cannot be neglected. We now enquire if the arbitrary assumptions in this preliminary modeling can be removed.

Table 2
Values for best-fit parameters

Best-fit parameter	Value
k_4 (s^{-1})	$(2.5 \pm 0.3) \times 10^5$
k_6 ($M^{-1}\,s^{-1}$)	$(2.1 \pm 0.8) \times 10^9$
$k_7 = k_8$ ($M^{-1}\,s^{-1}$)	$(1.2 \pm 0.7) \times 10^{10}$
σ	0.87 ± 0.02
β	0.55 ± 0.15

3.3.3. Best-fit parameters

Further analysis revealed that when considering the consumption of $^3CV^+$, reaction (6) predominates over (5). This arises because the formation of $^3CV^+$ in (3a) does not result in a high enough concentration of $^3CV^+$ to make reaction (5) significant in comparison to reaction (6). Thus, the calculated curves were the same whether k_5 was set equal to the initially assumed 1×10^{10} or $0\,M^{-1}\,s^{-1}$. We, therefore, omitted reactions (5a) and (5b) in further calculations. Since k_1, k_2 and k_3 are known this leaves only k_4, k_6, k_7 (=k_8), σ and β as possible best-fit parameters. Allowing these to be freely adjustable gave the final values shown in Table 2.

The calculated curves in this case were very similar to those shown in Fig. 3, but the $s_{\Delta A}$ is slightly lower (=2.4×10^{-3} compared to 3.0×10^{-3} for the data shown in Fig. 3), so the fit is slightly better. The errors shown for the best-fit parameters reflect the amount by which the parameter must be increased/decreased to double the value of $s_{\Delta A}$ from its best-fit value.

3.3.4. Thermochemical consideartions in the choice of reactions

The oxidation potentials of An and CV^+ versus the SCE are +1.16 and +0.80 V, respectively [17,24]. The corresponding reduction potentials are −1.93 and −0.79 V [17,25]. The triplet energies of An and CV^+ are 1.85 and 1.69 V. Using a Rehm–Weller type equation [26,27]

$$\Delta G_{et} = [E^{ox}\left(D^{\bullet+}/D\right) - E^{red}(A/A^{\bullet-})] - E_{0,0}$$

This allows us to determine the following DG's:

$$^3An + CV^+ \rightarrow An^{\bullet+} + CV^{\bullet}, \quad \Delta G = +0.1\,V \qquad (3b)$$

$$^3An + CV^+ \rightarrow An^{\bullet-} + CV^{\bullet 2+}, \quad \Delta G = +0.88\,V \qquad (9)$$

$$^3CV^+ + CV^+ \rightarrow CV^{\bullet} + CV^{\bullet 2+}, \quad \Delta G = -0.1\,V \qquad (6b)$$

$$^3CV^+ + An \rightarrow CV^{\bullet} + An^{\bullet+}, \quad \Delta G = +0.26\,V \qquad (10a)$$

$$^3CV^+ + An \rightarrow CV^{\bullet 2+} + An^{\bullet-}, \quad \Delta G = +1.04\,V \qquad (10b)$$

The more favorable thermochemistry of the first reaction compared to the second is the reason that we chose the first for the electron transfer reaction (3b). Its slightly endoergic nature is consistent with the fact that electron transfer accounts for only 13% of the overall reaction. Comparison of the thermochemistry of the last three reactions governed our choice of reaction (6b) as the most favorable second-order electron transfer reaction for $^3CV^+$.

3.3.5. General mechanistic comments

We can now make some general comments on the mechanism. As discussed above, rate constant k_3 controls the slope of the initial bleach. For $[CV^+]_0 = 16.81 \times 10^{-6}$ M, at maximum bleaching $\Delta A_{exp} \sim -0.12$ (Fig. 3). Since $\varepsilon_{590}(CV^+) = 9.7 \times 10^4\,M^{-1}\,cm^{-1}$, the concentration of bleached CV^+ in the 1 cm cell is ∼7% of the initial concentration. The bleached material is in the form of $^3CV^+$ and CV·, predominantly the former at the early stages. At the maximum bleach (curve minimum in Fig. 3), the rates of formation and consumption of $^3CV^+$ should be about equal. This can be confirmed as follows. Rate of formation of $^3CV^+$ at time $t = k_3{}^3An_t[CV^+]_t \leq k_3[^3An]_0[CV^+]_0 =$ 1.84E10 × 2.4E − 6 × 16.81E − 6 = 0.74 M s^{-1}. Rate of consumption of $^3CV^+ \approx k_4[^3CV^+]_t \approx k_4 \Delta E_{exp,t}/\varepsilon_{590} =$ 2.5E5 × 0.11/9.7E4 = 0.28 M s^{-1}.

The initial recovery of $^3CV^+$ back to CV^+ is controlled mainly by reaction (4) rather than by (6), because $k_4 = 2.5 \times 10^5\,s^{-1}$ while — even at the highest CV^+ concentration — $k_6\,[CV^+] = 2.1 \times 10^9\,(M^{-1}\,s^{-1}) \times 16.8 \times 10^{-6}\,(M) = 0.35 \times 10^5\,s^{-1}$. However, reactions (6b) and (3b) are important as the source of radicals. These radicals act as a reservoir of CV material, which is the source for the slow recovery of CV^+. Because of the relatively low radical concentrations this recovery is relatively slow even although the radical–radical reactions ((7) and (8)) proceed at close to diffusion controlled rate.

The value of the decay constant k_4 indicates that the lifetime of $^3CV^+$ in acetonitrile is short. Comparison of this lifetime with the previously determined phosphorescence lifetime, 0.29 s in solid matrix [11], suggests that on passing from a solid matrix to a solution of low viscosity a competitive rapid non-radiative decay brought about by conformational changes and rotational modes becomes possible.

The above parameters also resulted in good fitting of the model and experimental data obtained by varying the laser energy from 2 to 6 mJ for $[CV^+] = 16.81 \times 10^{-6}$ M, (0–100 ms). Bleach recovery curves, $[CV^+] = 1.68 \times 10^{-5}$ M, similar to that shown in Fig. 3 were also obtained at the monitoring wavelengths 520, 540, 560, 590 and 605 nm. These results suggest that triplet sensitization of CV^+ results in population of a triplet state, which decays to a normal ground-state conformation.

In an earlier report on the quenching of ^3An in acetonitrile by CV^+, we interpreted our results in terms of energy transfer [13]. The present study provides a convenient method for determining both energy transfer and electron transfer and show that, although energy transfer is the dominant channel, there is a substantial amount of electron transfer (13%). In this respect, it is interesting to note that Bhasikuttan et al. [19] have also interpreted their results for the $^3An/CV^+$ system in benzene only in terms of energy transfer. If this is correct then the percentage of energy transfer relative to

electron transfer is solvent dependent. Moreover, in studying the interaction of dyes (crystal violet, phenosafranine, methylene blue) in acetonitrile with triplet benzophenone (^{3}Bp), Jockusch et al. [28] reported that for ^{3}Bp/CV$^+$ electron transfer occurred while triplet transfer was dominant in the other two cases. It would seem possible that in triarylmethane dye systems both energy transfer and electron transfer are occurring and that fitting the bleach/recovery data allows a rather sensitive determination of the percentage of each channel.

Acknowledgements

Financial support from Polaroid Corporation is greatly appreciated.

References

[1] D.F. Duxbury, Chem. Rev. 93 (1993) 381.
[2] D. Magde, M.W. Windsor, Chem. Phys. Lett. 24 (1974) 144.
[3] D.A. Cremers, M.W. Windsor, Chem. Phys. Lett. 71 (1980) 27.
[4] R. Menzel, C.W. Hoganson, M.W. Windsor, Chem. Phys. Lett. 120 (1985) 29.
[5] V. Sundstrom, T. Gilbro, H. Bergstrom, Chem. Phys. 73 (1982) 439.
[6] M. Vogel, W. Rettig, Ber. Bunsenges. Physik. Chem. 89 (1985) 962.
[7] T. Forster, G. Hoffman, Z. Physik. Chem. NF 75 (1971) 63.
[8] Y.M.A. Naguib, S.G. Cohen, C. Steel, J. Am. Chem. Soc. 108 (1986) 128.
[9] G. Oster, G. Oster, in: H.P. Kallman, G. Marmor-Spruch (Eds.), Luminescence of Organic and Inorganic Materials, Wiley, New York, 1962, p. 186.
[10] C. Nouchi, C.R. Silvie, C.R. Acad. Sci. Ser. A, B 268B (1969) 546.
[11] I. Leaver, Photochem. Photobiol. 16 (1972) 189.
[12] G. Jones, K. Goswami, J. Photochem. Photobiol. A: Chem. 57 (1991) 65.
[13] Y.M.A. Naguib, C. Steel, S.G. Cohen, M.A. Young, J. Photochem. Photobiol. A: Chem. 96 (1996) 149.
[14] H. Linschitz, C. Steel, J.A. Bell, J. Phys. Chem. 66 (1962) 2574.
[15] N.J. Turro, Modern Molecular Photochemistry, University Science Books, Mill Valley, CA, 1991, p. 344.
[16] R. Bensasson, E.J. Land, Trans. Faraday Soc. 67 (1971) 1904.
[17] G.J. Kavarnos, N.J. Turro, Chem. Rev. 86 (1986) 401.
[18] J.A. Barltrop, J.D. Coyle, Excited States in Organic Chemistry, Wiley, New York, 1975, p. 130.
[19] A.C. Bhasikuttan, L.V. Shastri, A.V. Sapre, J.P. Mittal, J. Photochem. Photobiol. A: Chem. 112 (1998) 179.
[20] A.J. Paine, R. Loutfy, Rev. Chem. Intermed. 5 (1984) 227.
[21] J.H. Noggle, Physical Chemistry on a Microcomputer, Little Brown, Boston, 1985 (Chapter 8).
[22] W.H. Press, B.P. Flannery, S.A. Teukolsky, W.T. Vetterling, Numerical Recipies: The Art of Scientific Computing, Cambridge University Press, Cambridge, 1986 (Chapter 10).
[23] S.A. Naman, L. Tegner, Photochem. Photobiol. 43 (1986) 331.
[24] Z. Calus, R.N. Adams, J. Am. Chem. Soc. 84 (1962) 3207.
[25] H. Volz, W. Lotsch, Tetrahedron Lett. (1969) 2275.
[26] D. Rehm, A. Weller, Isr. J. Chem. 8 (1970) 259.
[27] A. Gilbert, J. Baggott, Essentials of Molecular Photochemistry, CRC Press, Boca Raton, FL, 1991, p. 160.
[28] S. Jockusch, H.J. Timpe, Ch.H. Fischer, W. Schnabel, J. Photochem. Photobiol. A: Chem. 63 (1992) 217.